Journal of Materials Chemistry A

PAPER

View Article Online
View Journal | View Issue

Cite this: J. Mater. Chem. A, 2014, 2, 18293

Interfacially reinforced unsaturated polyester composites by chemically grafting different functional POSS onto carbon fibers†

Dawei Jiang,[ab] Lixin Xing,[a] Li Liu,*[a] Xingru Yan,[b] Jiang Guo,[bc] Xi Zhang,[b] Qingbo Zhang,[a] Zijian Wu,[a] Feng Zhao,[a] Yudong Huang,[a] Suying Wei*[bc] and Zhanhu Guo*[b]

Monofunctional (methacrylolsobutyl) and multifunctional (methacryl) polyhedral oligomeric silsesquioxane (POSS) were successfully grafted on a carbon fiber (CF) surface to enhance the interfacial strength of CF reinforced unsaturated polyester resin (UPR) composites. The silicon containing functional groups were obviously increased on the CFs after the successful grafting of POSS onto the CF surface. Both kinds of POSS were uniformly grafted on the CF surface and the surface roughness of the CFs grafted with methacryl POSS and methacrylolsobutyl POSS was almost the same (131.6 and 129.6 nm) but much higher than that of the as-received CFs (57.9 nm). Dynamic contact angle analysis of the CFs grafted with both POSS showed almost the same surface energy but higher than that of the as-received CFs. After being grafted with methacrylolsobutyl POSS, the interlaminar shear strength of the composites was 62 MPa, increased by 31.9%, however, in terms of methacryl POSS the value was 67 MPa, increased by 42.6% compared with that of the as-received CFs (47 MPa). The interfacial shear strength (IFSS) of the composites with methacryl POSS grafted CFs (93 MPa) was significantly increased by 102.2% compared with the composites with the as-received CFs (46 MPa) and is even higher than that of the composites with methacrylolsobutyl POSS grafted CFs (87 MPa). The impact energy of 1.72 J for the composites with methacryl POSS grafted CFs is higher than that of the composites with as-received CFs (1.00 J) and methacrylolsobutyl POSS grafted CFs (1.43 J).

Received 6th August 2014
Accepted 8th September 2014

DOI: 10.1039/c4ta04055d

www.rsc.org/MaterialsA

Introduction

Owing to their high modulus, strong tensile strength, low density, excellent chemical resistance, high temperature tolerance and low thermal expansion, carbon fibers (CFs) have been widely deployed in aerospace, marine and automobile industries,[1–4] mainly serving as reinforcements in composites such as CF reinforced polymer or carbon composites.[5,6] The combination of CFs and polymer often gives rise to high strength materials with minimum weight for structural composites.[7,8] The CF reinforced polymer matrix composites normally contain three parts including reinforcing CFs, the hosting matrix and the interphase between CFs and the matrix. The mechanical properties of the CF reinforced composites depend not only on the intrinsic characteristics of the fibers and of the matrix but also on the physicochemical properties of the interphase. This interface between the fiber and the matrix makes a critical contribution to the performance of the composites and a poor quality interface can result in poor mechanical properties.[9–11] CFs are known to have smooth and inert characteristics of carbon that hardly react with the active groups of the polymer matrix. In addition, the poor wettability between CFs and the polymer can result in weak interfacial adhesion between fibers and the matrix.[12] Both physical coating treatment[13,14] and chemical grafting[15–18] have been reported to increase the surface wettability, surface roughness or chemical bonding aiming to increase the interfacial strength between CFs and the matrix.

Though the interphase and various reinforcement mechanisms have been reported on the CFs/epoxy composites,[16,19–21] the effects of interphase on the CF reinforced unsaturated polyester resin (UPR) composites and the factors influencing the interface between CFs and UPR have not been reported so far. There is a lack of understanding on how to obtain a "successful interface" between CFs and UPR, that is, how to increase the interfacial strength as high as possible is not clear. UPRs have been widely used in the composite industry for decades due to their ease of processing, relatively low cost,

[a]School of Chemical Engineering and Technology, Harbin Institute of Technology, Harbin, 150001, China. E-mail: liuli@hit.edu.cn; Tel: +86-1393669907

[b]Integrated Composites Laboratory (ICL), Dan F Smith Department of Chemical Engineering, Lamar University, Beaumont, TX 77710, USA. E-mail: zhanhu.guo@lamar.edu; Tel: +1(409) 880-7654

[c]Department of Chemistry and Biochemistry, Lamar University, Beaumont, TX 77710, USA. E-mail: suying.wei@lamar.eud; Tel: +1(409) 880-7976

† Electronic supplementary information (ESI) available. See DOI: 10.1039/c4ta04055d

excellent mechanical properties, good chemical and weather resistance.[22,23] UPRs are thermosetting materials with low curing temperature, which can be easily made with CFs to form reinforcement composites. CF reinforced UPR composites are based on the use of reinforcement to improve the mechanical strength of UPRs, which can be applied to various areas, including automotives, architecture, aircrafts and the chemical industry. The fiber reinforcements can effectively improve the mechanical strength and hardness of the composites. However, a poor interfacial strength between CFs and UPR was observed to result in a low interlaminar shear strength and interfacial shear strength for the CF reinforced UPR composites.[24]

Polyhedral oligomeric silsesquioxane (POSS) possesses hybrid organic–inorganic composition with an inorganic central core $(SiO_{1.5})_n$ providing thermal and chemical stability, and the surrounding inorganic cage with eight organic groups that can be functionalized with non-reactive groups for an enhanced compatibility with the hosting polymer matrix or with the functional groups for chemically reacting with a polymer matrix.[25–27] POSS is the smallest known silica particle with a three-dimensional Si–O cage structure and an overall diameter of 1.5–3 nm.[28,29] Our previous work has demonstrated the ability of POSS to increase the roughness and wettability of the CFs when incorporated through grafting onto a CF surface.[30] The experiment has verified that the roughness rather than the wettability played a more important role on the interface of CF reinforced UPR composites. However, there was still a limited increase of the interfacial strength of the composites. The hydrogen bonding interaction and miscibility behavior between polymers and POSS can be controlled by varying the organic groups. The introduction of POSS cages can improve the mechanical properties of the composites including strength, modulus and rigidity through improving the interface adhesion of the composites. The introduced POSS can also reduce the flammability of the final finishing, heat evolution, and viscosity during processing.[31–34] Efforts to greatly enhance the mechanical properties of the CF reinforced UPR composites and to figure out the factors in determining the interfacial strength of the composites are emergent and important targets. However, to reinforce CFs/UPR composites through introducing exotic strong units such as POSS with different functional groups could be an alternative to further improve the interfacial strength of CF reinforced composite and has not been reported yet.

In this paper, monofunctional POSS and multifunctional POSS with eight functional groups were first introduced into CFs using a silane coupling agent by chemical grafting to enhance the interfacial properties. The CFs with and without surface treatment were used to obtain the CF reinforced UPR composites by compression molding. And the effects of the chemical bonding on the interface of CFs/UPR composites have been investigated. The surface functional groups and surface chemical composition of CFs were characterized by Fourier transform infrared spectroscopy (FTIR) and X-ray photoelectron spectroscopy (XPS), respectively. The surface morphologies of the CFs were observed by atomic force microscopy (AFM). The wettability and surface free energy of the untreated and functionalized fibers were investigated by the dynamic contact angle analysis test (DCAT). The interfacial mechanical properties of the composites were characterized by the short-beam bending test method (interlaminar shear strength, ILSS), the single fiber pull-out test method (interfacial shear strength, IFSS) and the impact test method (impact toughness). The micro-mechanism of the composite interphase region was investigated by force modulation atomic force microscopy (FMAFM).

Experimental section

Materials

AROPOL MR13006 unsaturated polyester resin (UPR) and low shrinkage agent LP4016 (reducing the volume shrinkage of UPR curing) were supplied by Ashland Inc., USA. MR13006 is a copolymer of propanediol, maleic anhydride and phthalic anhydride, number-average molar mass (M_n) is 2400 g mol^{-1}, weight-average molecular weight (M_w) is 5200 g mol^{-1}, and the polydispersity (M_w/M_n) is 2.20. The main component of low shrinkage agent LP4016 is polyvinyl acetate (M_n = 38 900 g mol^{-1}, M_w = 99 300 g mol^{-1}, and M_w/M_n = 2.55). *tert*-Butyl peroxybenzoate (TBPB, 98% purity, ACROS ORGANICS Inc.) was used as an initiator for UPR curing. Benzoyl peroxide (BPO, 75% remainder water from Sigma-Aldrich) was used for grafting. $NaBH_4$ (98% purity) was purchased from Alfa Aesar. H_2SO_4 (98%) and HNO_3 (68%) were purchased from Tianjin Dongli big chemical reagent factory. Un-sizing polyacrylonitrile (PAN) based carbon fibers (Chinese Carbon Fiber 300, CCF300) were obtained from WeiHai GuangWei Group (12×10^3 single filaments per tow, tensile strength of 3.26 GPa, average diameter of 7 μm, density of 1.76 g cm^{-3}, Shandong, China). Methacryl and methacrylolsobutyl POSS were obtained from Hybrid Plastics Co., Inc. and were used as received. 3-(Methylacryloxyl)propyltrimethoxy silane (KH570) coupling agent as an intermediate product was obtained from Wuhan Chenxi Chemical Co., Ltd. The chemical structures of POSS, BPO, TBPB, KH570, UPR and un-sizing CFs are shown in Fig. 1.

Grafting procedures of POSS

The CFs (4 g) were oxidized in a 3 : 1 (v/v) mixture of concentrated H_2SO_4/HNO_3 at 60 °C for 2 h and washed with deionized water until water was neutral. The oxidized CFs were then reduced in a solution of $NaBH_4$ (1.0 g) in 200 mL anhydrous ethanol at room temperature for 20 h. The mixture was heated to 78 °C and maintained for 4 h. The products were washed with deionized water until the solution became neutral and then dried (the product is denoted as "CF–OH"). The reduced CFs were soaked into a mixture solution of 4 mL KH570 and 96 mL ethanol at room temperature for 30 min, and then the temperature was increased and maintained at 78 °C for 5 h. The CFs were washed with absolute ethanol for 5 times to remove the unreacted KH-570. And then, the CFs were put into an oven at 80 °C for 4 h (the product is denoted as "CF–C═C"). After being grafted with KH570, the CFs were reacted with methacryl POSS or methacrylolsobutyl POSS in 50 g methylbenzene

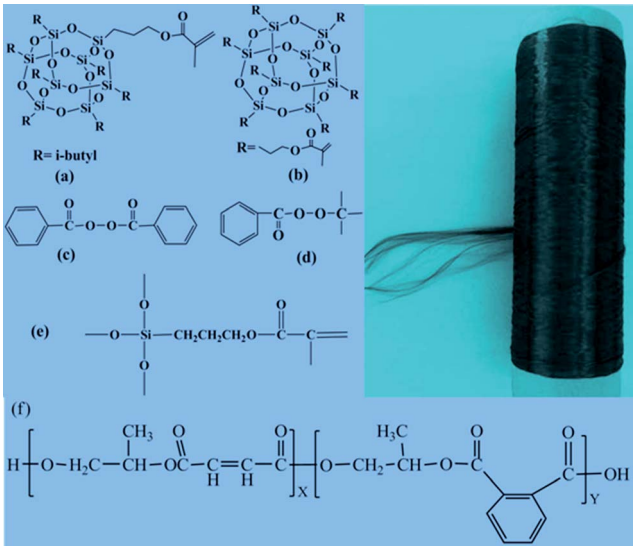

Fig. 1 Chemical structures of (a) methacrylolsobutyl POSS, (b) methacryl POSS, (c) BPO, (d) TBPB, (e) KH570, and (f) UPR; and the image of the un-sizing CFs.

solutions of 1 g methacryl POSS with 0.2 g BPO or 1 g methacrylolsobutyl POSS with 0.2 g BPO at 110 °C for 7 h, respectively. The product was rinsed with excess methylbenzene to remove unreacted POSS and BPO, washed with deionized water until water became neutral, and then dried for other usages (the product is denoted as "CF–POSS"). The grafting of POSS on the surface of CFs is shown in Fig. 2.

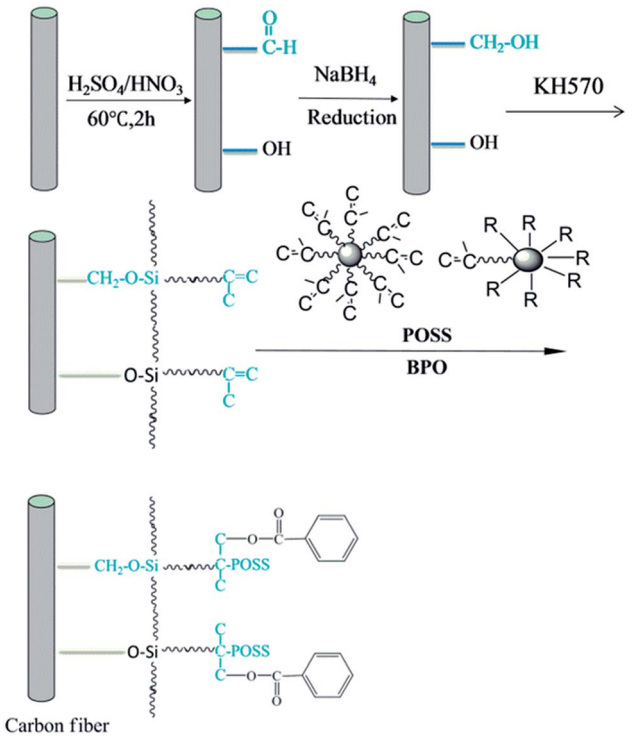

Fig. 2 Schematic of the grafting procedures of POSS grafted carbon fibers.

Fabrication of CFs/UPR composites

The composites of CF reinforced UPR were prepared by the compression molding method. The unidirectional prepreg carbon fibers were put into a mold to make composites. MR13006, LP4016 and TBPB were used at a mixture ratio (weight) of 105 : 45 : 1. Briefly, the CFs/UPR composites were prepared by heating the samples at 80 °C for one hour without pressure, a pressure of 10 MPa was applied at 100 °C for one hour, then the sample was heated at 140 °C for one hour under 10 MPa, and finally the mold was cooled down to room temperature with the pressure being maintained. The resin content of the composites was controlled at 30 ± 1.5 mass%, and the width and thickness of specimens were 6.5 and 2 mm, respectively.

Characterization

The surface functional groups of the CFs were analyzed using a Fourier Transform Infrared (FTIR) spectrophotometer (Nicolet, Nexus 670, USA) in Attenuated Total Reflectance (ATR) mode. Before the surface analysis, the CFs were dried for 2 h under vacuum at 150 °C. In order to obtain a good optical contact, a very thin KBr layer was introduced between the prism and the CFs by using a KBr pelletizer. The FTIR spectra were acquired by scanning the specimens 64 times in the wavenumber range of 400–4000 cm^{-1} with the resolution of 2 cm^{-1}.

X-ray photoelectron spectroscopy (XPS, ESCALAB 220iXL, VG, UK) was carried out to study the surface element of CFs using a monochromated Al Kα source (1486.6 eV) at a base pressure of 2×10^{-9} mbar. The XPS was energy referenced to the C1s peak of graphite at 284.6 eV. The XPS Peak version 4.1 program was used for data analysis. The treatment effects on the fiber surface morphology were observed by using atomic force microscopy (AFM, Solver-P47H, NT-MDT, Russia). An individual fiber was examined in a Solver P47 AFM/STM system (NT-MDT Co.). AFM was also used to investigate the microstructures of the composites. The force modulation mode was adopted to study the cross-section surfaces of unidirectional CFs/UPR composites and the relative stiffness of the various phases, including the CFs, interface, and resin. The composites were first polished perpendicularly to the fiber axis using increasingly finer sand papers, and then with a Cr_2O_3 (50 nm) suspension, finally washed with water under ultrasonication and dried for tests.

Dynamic contact angle and surface energy analyses between testing liquids and single fiber were performed using a dynamic contact angle tensiometer (DCAT21, Data Physics Instruments, Germany).

The interlaminar shear strength (ILSS) of the CFs/UPR composites was measured on a universal testing machine (WD-1, Changchun, China) using a three point short beam bending test according to ASTM D2344. Specimen dimensions were 20 mm × 6.5 mm × 2 mm, with a span to thickness ratio of 5. The specimens were conditioned and an enclosed testing space was

maintained at room temperature. The measurements were at a cross-head speed of 2 mm min^{-1}.

The impact tests were carried out in a drop weight impact test system (9250HV, Instron, USA). The specimen dimensions were 55 mm × 6.5 mm × 2 mm, the impact span was 40 mm, the drop weight was 3 kg and the velocity was 2 m s^{-1}. Each reported data set was an averaged value of 5 specimens. The interfacial shear strength (IFSS) was adopted to quantify the interfacial property between CFs and the resin matrix by the interfacial evaluation equipment (Tohei Sangyo Co. Ltd., Japan). The illustration of the single fiber-micro-bond test is shown in Fig. S1† and the testable embedded length of the resin droplet is around 50 μm. The curing procedure was the same as that for the preparation of CFs/UPR composites.

The tensile strength (TS) of a single filament was performed on an electronic mechanical universal material testing machine (Instron 5500R, USA) according to ASTM D 3379-75. A gauge length of 20 mm and a cross-head speed of 10 mm min^{-1} were used for all fiber samples. At least, 60 specimens were tested for each fiber type, and then the average value was considered as the tested value.

Results and discussion

Surface chemical elemental and topography of carbon fibers

The FTIR spectra can provide precise information of the material surface functional groups even at low concentrations.[35] FTIR-ATR is a sensitive technique for surface functional group analysis of CFs.[20] Fig. 3(a–c) show the FTIR spectra of the as-received, methacryl POSS grafted and methacrylolsobutyl POSS grafted CFs. The untreated CFs are observed to have the bending vibration of adsorbed water on the fiber surface at 3430 cm^{-1} and the bands at around 2930 and 2850 cm^{-1} can be assigned to the C–H stretching of methyl and methylene groups. No other organic groups are observed in the as-received fibers, Fig. 3(a). For the POSS grafted CFs, some other bands appeared except the original peaks on the CF surface. The broad band at about 880–800 cm^{-1} corresponds to the Si–C stretching vibration, Fig. 3(b and c). The bands at 1020 and 1050 cm^{-1} for the methacryl POSS grafted and methacrylolsobutyl POSS grafted CFs correspond to Si–O–Si stretching vibrations, respectively. The band at 1100 cm^{-1} was assigned to the stretching vibration of C–O–C. The band at 1270 cm^{-1} corresponded to the asymmetric deformation vibration of the CH_2 of Si–CH_2 due to the grafted POSS. These results show that the surface grafting of methacryl POSS and methacrylolsobutyl POSS were successful on the CFs.

The surface composition of the as-received and grafted CFs was determined by XPS[36] and the results are shown in Table 1. Only carbon, oxygen and a small amount of nitrogen were observed on the as-received CF surface. After being grafted with methacrylolsobutyl and methacryl POSS, the composition was changed. The carbon content was decreased from 82.03% for the as-received CFs to 67.47 and 71.66% and the oxygen content was increased from 16.86% for the as-received CFs to 23.14 and 21.65% for the methacryl POSS and methacrylolsobutyl POSS grafted CFs, respectively. The O/C value for the methacryl POSS and methacrylolsobutyl POSS grafted CFs was higher than that of the as-received CFs and the silicon was observed with an element content of 8.25 and 5.46%, respectively. The surface atomic Si/C ratios were increased sharply from 0 to 0.12 and 0.08 for the methacryl POSS and methacrylolsobutyl POSS

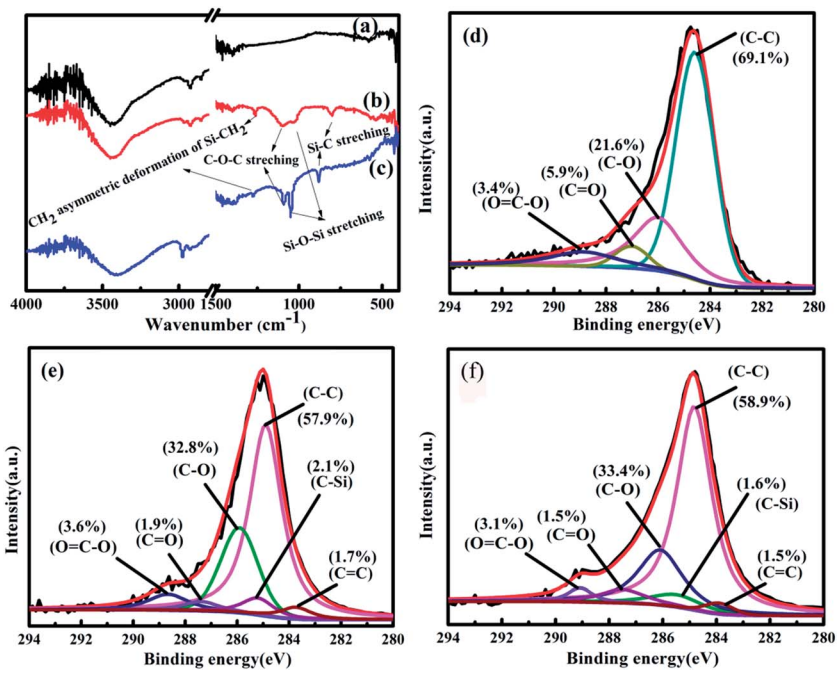

Fig. 3 FTIR-ATR and C1s XPS spectra of the (a and d) as-received, (b and e) methacryl POSS grafted and (c and f) methacrylolsobutyl POSS grafted CFs.

Table 1 Surface chemical composition of CFs with and without POSS grafting

	Elemental content (at.%)					
Carbon fibers	C	O	N	Si	O/C	Si/C
As-received CFs	82.03	16.86	1.1	—	0.20	—
CF–methacryl POSS	67.47	23.14	1.14	8.25	0.34	0.12
CF–methacrylolsobutyl POSS	71.66	21.65	1.23	5.46	0.30	0.08

grafted CFs, indicating that the POSS had been successfully grafted on the CF surface.

The C1s XPS spectra of the as-received and methacryl POSS and methacrylolsobutyl POSS grafted CFs are shown in Fig. 3(d–f). The C1s spectrum of the as-received CFs shows 69.1% C–C, 21.6% C–O, 5.9% C═O and 3.4% O–C═O. The C1s spectra of the methacryl POSS and methacrylolsobutyl POSS grafted CFs exhibit 57.9 and 58.9% C–C, 32.8 and 33.4% C–O, 1.9 and 1.5% C═O, 3.6 and 3.1% O–C═O, 2.1 and 1.6% C–Si, and 1.7 and 1.5% C═C, respectively. Compared with the as-received CFs, the C–O was increased significantly from 21.6 to 32.8 and 33.4% for the methacryl POSS and methacrylolsobutyl POSS grafted CFs, respectively, and the C–Si and C═C were observed due to the introduced methacryl POSS and methacrylolsobutyl POSS on the CF surface, consistent with the results of the XPS survey spectra discussed above.

Fig. 4 shows the AFM 3-dimensional images of the as-received methacryl POSS and methacrylolsobutyl POSS grafted CFs. The carbon fiber surface roughness, calculated from the plane topography images by using the AFM software, is shown in Table 2. Significant differences of the surface topography between the as-received and grafted CFs were observed. Fig. 4(a) shows the surface of the as-received CFs with many relatively neat shallow grooves arising from the production process, a typical topography of the used CFs. Because of the neat surface, the as-received CFs have a small roughness with a value of 57.9 nm, however, the surface of CFs grafted with methacryl POSS and methacrylolsobutyl POSS becomes much rougher due to a layer of uniform POSS particles scattered on the surface and in the voids of the fiber grooves, Fig. 4(b and c). For the methacryl POSS and methacrylolsobutyl POSS grafted CFs, almost the same surface roughness of 131.6 and 129.6 nm is observed. The roughness of the CFs grafted with the methacryl POSS and methacrylolsobutyl POSS was calculated to be increased by 127 and 124%, respectively. The increased surface roughness could provide more interlocking points and friction between CFs and the matrix, and thus could enhance the mechanical interlocking between CFs and the matrix, a similar phenomenon was also observed in the epoxy nanocomposites with graphene nanosheets anchored with metal nanoparticles.[37] With the increase of the surface roughness, the interfacial adhesion of the resulting composites was improved.

Dynamic contact angle analysis

It is well known that the surface functionality and roughness of the CFs can affect the fiber surface energy.[38,39] High fiber surface energy could promote a better wettability between CFs and the matrix to increase the integrative performance of the CF reinforced resin composites. The surface wettability of the CFs was evaluated by the surface free energy. The overall performance of the fiber-reinforced composites is closely related to the wettability of the fiber surface with the matrix. An excellent wettability means a high interfacial strength. Generally, the CFs should be pre-treated before their usage as reinforcement aiming to obtain fibers with a surface energy higher or equal to that of the matrix for the improvement of wettability.

The advancing contact angle was determined from the mass change during the immersion of fibers in each test liquid, using Wilhelmy's eqn (1):[40]

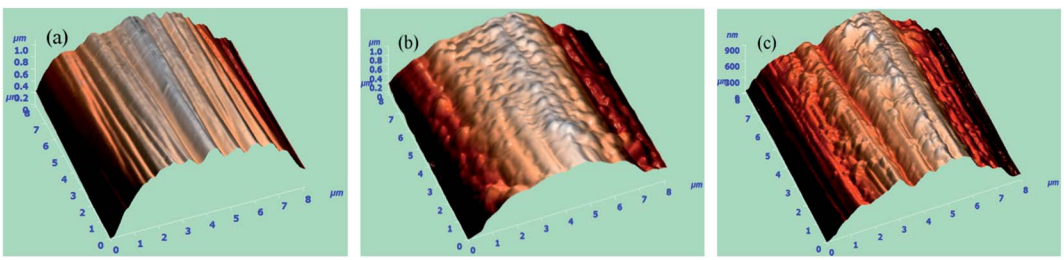

Fig. 4 AFM three-dimensional images of the (a) as-received CFs, (b) methacryl POSS grafted CFs, and (c) methacrylolsobutyl POSS grafted CFs.

Table 2 Contact angle, surface energy and roughness of CFs with different chemical grafting

	Contact angle (°)		Surface energy (mJ m^{-1})			
CF	Water	Diiodomethane	γ^d	γ^p	γ	Ra (nm)
As-received CFs	74.39	56.31	23.82	10.64	34.46	57.9
CF–methacryl POSS	66.36	53.35	32.39	11.70	44.09	131.6
CF–methacrylolsobutyl POSS	67.68	54.13	31.94	11.14	43.08	129.6

$$\cos\theta = \frac{mg}{\pi d_f \gamma_1} \quad (1)$$

where, d_f is the fiber diameter, g is the gravitational acceleration, and γ_1 is the surface energy of the test liquid. The surface energy (γ_f), dispersion component (γ_f^d) and polar component (γ_f^p) of the CFs were estimated from the measured dynamic contact angles of the test liquids with known surface tension components and were calculated according to eqn (2) and (3):

$$\gamma_1(1 = \cos\theta) = 2(\gamma_1^p\gamma_f^p)^{1/2} + 2(\gamma_1^d\gamma_f^d)^{1/2} \quad (2)$$

$$\gamma_f = \gamma_f^p + \gamma_f^d \quad (3)$$

where, γ_1, γ_1^d and γ_1^p are the liquid surface energy, its dispersion and polar component, respectively. Deionized water (γ^d = 21.8 mJ m^{-1}, γ = 72.8 mJ m^{-1}) and diiodomethane (γ^d = 50.8 mJ m^{-1}, γ = 50.8 mJ m^{-1}, 99% purity, Alfa Aesar, USA) were used as the test liquids. Each measurement was repeated 5 times and the results were averaged. In this work, the surface wettability of CFs was evaluated *via* a Cahn dynamic angle analysis system. The θ, γ, γ^d and γ^p of the as-received and grafted CFs are summarized in Table 2. Fig. 5 shows the principle of the contact angle for a single fiber. As shown in Table 2, the θ of the as-received CFs with polar water and non-polar diiodomethane was 74.39 and 56.31°, respectively, the γ was 34.46 mJ m^{-1}, and the γ^d and γ^p were 23.82 and 10.64 mJ m^{-1}, respectively. After grafting with methacryl POSS and methacrylolsobutyl POSS, the θ was decreased to 66.36 and 67.68° from 74.39° for polar water, and decreased to 53.35 and 54.13° from 56.31° for non-polar diiodomethane. The γ_f obviously increased and its γ^d and γ^p components of methacryl POSS grafted CFs were 32.39 and 11.70 mJ m^{-1}, respectively. The γ^d and γ^p for methacrylolsobutyl POSS grafted CF were calculated to be 31.94 and 11.14 mJ m^{-1}, similar to that of the methacryl POSS CFs. The γ_f of the methacryl POSS grafted CFs was calculated to be 44.09 mJ m^{-1}, slightly higher than that of the methacrylolsobutyl POSS grafted CFs (43.08 mJ m^{-1}). The increased surface energy of CFs could effectively improve the wettability between the fibers and the resin, and simultaneously increase the interfacial strength. After being grafted with both kinds of POSS, the γ_f of the CFs was almost the same and larger than that of the as-received CFs.

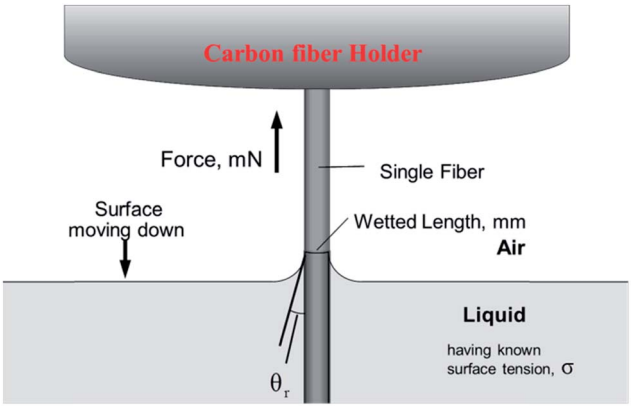

Fig. 5 Sketch of the receding contact angle for a single carbon fiber.

Interfacial property testing

Direct force modulation AFM (FMAFM) was applied to characterize the surface topography, adhesion, elasticity and hardness of the material surface. FMAFM images could reveal the existence of at least two clearly different configurations with different hardnesses and elastic area distributions within one material. Different components of composites have different performances due to their different stiffnesses among the fiber, matrix and interface area. Generally, different phases in FMAFM have different color contrasts, while different colors correspond to the variation in the modulus. The darker the color is, the higher the modulus is. The information of the shape, distribution and relative hardness of different phases (including interface phase) can be obtained from the FMAFM test to provide the basis for the mechanism analysis of interface modification.[41–44] The AFM images of the cross-section morphology and FMAFM images of the interface region between CFs and the UPR matrix are shown in Fig. S2† and 6.

The AFM cross-section morphology image of the UPR composites reinforced by CFs grafted with methacryl POSS is shown in Fig. S2.† Fig. S2† shows a uniform distribution between CFs and UPR in the composites, and the CF diameter is confirmed around 7 μm. The force modulation images of the interphase region between CFs and the UPR matrix were obtained from the cross-section of the composites reinforced by methacryl POSS and methacrylolsobutyl POSS grafted CFs, Fig. 6. Fig. 6(a–c) illustrate the interphase between CF and the UPR matrix. The clear interface region is observed, Fig. 6(b and c), however only two phases are observed between CF and the UPR matrix region for the composites, Fig. 6(a). These interfaces of the grafted CF reinforced UPR composites are observed to have a bridge-like morphology with a rough surface, and a homogeneous interface layer is observed between CFs and the UPR matrix. For the methacryl POSS grafted CF reinforced UPR composites, the interfacial transition region is observed longer and softer than that of the CFs grafted with methacrylolsobutyl POSS, due to the different molecular structures between methacryl and methacrylolsobutyl POSS, Fig. 6(b and c). The molecular structures of the methacryl and methacrylolsobutyl POSS have hybrid molecules with inorganic silsesquioxane at the core and organic groups attached at the corner of the cage. There are eight active methacrylate groups in the methacryl POSS, however, only one methacrylate group in the methacrylolsobutyl POSS. The longer and softer interface region for the methacryl POSS grafted CF reinforced UPR composites can be attributed to these active methacrylate groups that not only can be grafted on the CF surface through one of the eight methacrylate groups but also can react with the double bonds of UPR. However for the methacrylolsobutyl POSS grafted CF reinforced UPR composites, only one active methacrylate group can just be grafted on the CF surface without any reaction with UPR, Fig. 6(b and c). The methacryl POSS grafted CFs can provide good interfacial bonding strength by both the chemical

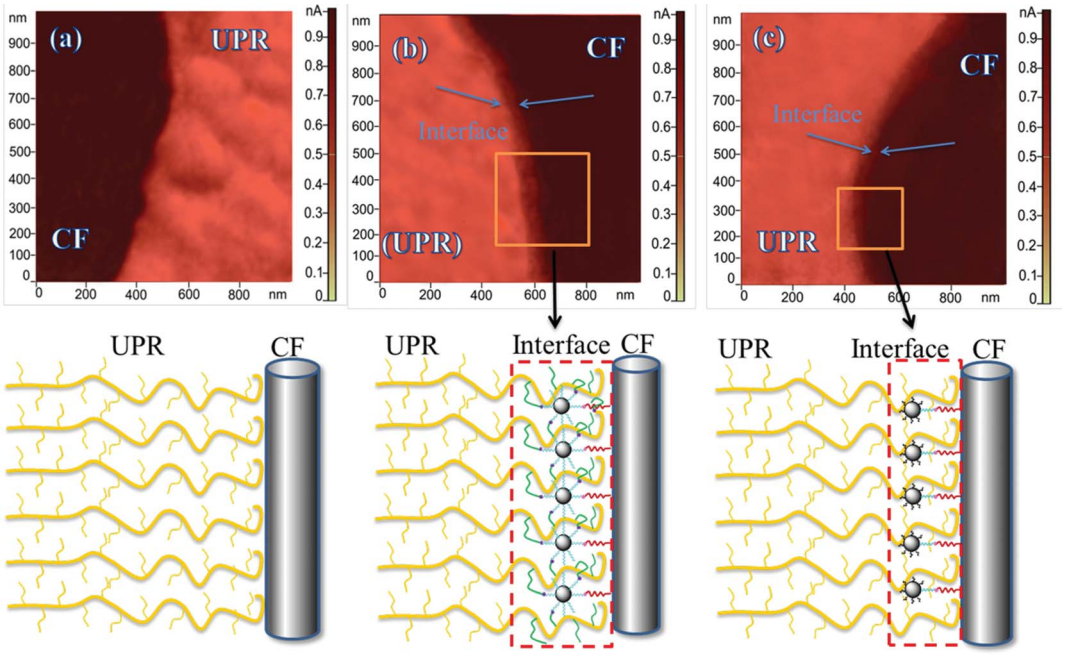

Fig. 6 (a–c) Force modulation AFM images and the sketch of as-received, methacryl POSS grafted and methacrylolsobutyl POSS grafted CFs for the CFs/UPR composites.

bonding to bridge the CFs and UPR and the mechanical interlocking of the CFs with the UPR matrix, a similar phenomenon has been reported for the epoxy nanocomposites reinforced with graphene nanosheets decorated with protruding nanoparticles.[37] The excellent interface region of composites can increase the out-of-plane mechanical performance of the composites and a longer interface region can decrease the applied force on the composites of CFs and UPR.

The out-of-plane mechanical performance of laminated composites is performed by inter-laminar shear stress defined at the interface between CFs and UPR in laminated composite materials. The interlaminar shear stresses are important since they have a significant effect on the failure strength of the composite laminate.[45–47] The interlaminar shear strength (ILSS, Γ) of the as-received and grafted CF reinforced UPR composites has been characterized by short-beam bending tests to evaluate the interfacial strength of the composites. The Γ for the short-beam test was calculated according to eqn (4).[48]

$$\Gamma = \frac{3P_b}{4bh} \quad (4)$$

where P_b is the maximum compression force at fracture in Newton, b is the width of the specimen in mm, and h is the thickness in mm. Each reported Γ value was averaged for more than eight successful measurements. Fig. 7(a) shows the ILSS of the as-received, methacryl and methacrylolsobutyl POSS grafted CF reinforced UPR composites. After being grafted with methacryl or methacrylolsobutyl POSS, the modified fiber composites possess better ILSS than that of the as-received fiber composites. The as-received CFs/UPR composites have an ILSS value of 47 MPa, as compared with methacryl POSS grafted CFs/UPR composites with a ILSS of 67 MPa, an increase of 42.6%. However, the methacrylolsobutyl POSS grafted CFs/UPR composites have an ILSS of 62 MPa, a little lower than that of the methacryl POSS grafted CFs/UPR composites and an increase of 31.9% compared with the as-received CFs/UPR composites. Zhao *et al.*[20] have reported that the ILSS of the epoxy composites was increased by 36.4% by grafting octaglycidyldimethylsilyl POSS and carbon nanotubes on the CF surface. Bekyarova *et al.*[49] have reported that the functionalized single-walled carbon nanotubes with carboxyl groups dispersed in epoxy for CFs/epoxy composites have an increased ILSS value by 40% than that of the untreated CFs. All of the percentage increase is lower than the observed ILSS value here with CFs grafted with methacryl POSS.

The improved interfacial strength for the methacryl POSS grafted CFs/UPR composites could be attributed to both the enhanced mechanical interlocking and the introduced chemical bonding at the interface of the composites. However, there is only mechanical locking at the interface of the methacrylolsobutyl POSS grafted CFs/UPR composites. The wettability and roughness of the modified CFs are nearly the same for the composites with methacryl and methacrylolsobutyl POSS grafted CFs. However, the difference of the interfacial strength improvements was due to the chemical bonding difference at the interface of the composites between methacryl and methacrylolsobutyl POSS grafted CFs. A similar trend and phenomenon were observed for the interfacial shear strength (IFSS). The IFSS was calculated according to eqn (5).

$$\mathrm{IFSS} = \frac{F_{\max}}{\pi \times d_f \times l_e} \quad (5)$$

where $F_{\max}$ is the maximum load recorded, d_f is the carbon fiber diameter, and l_e is the embedded length of the carbon fiber in

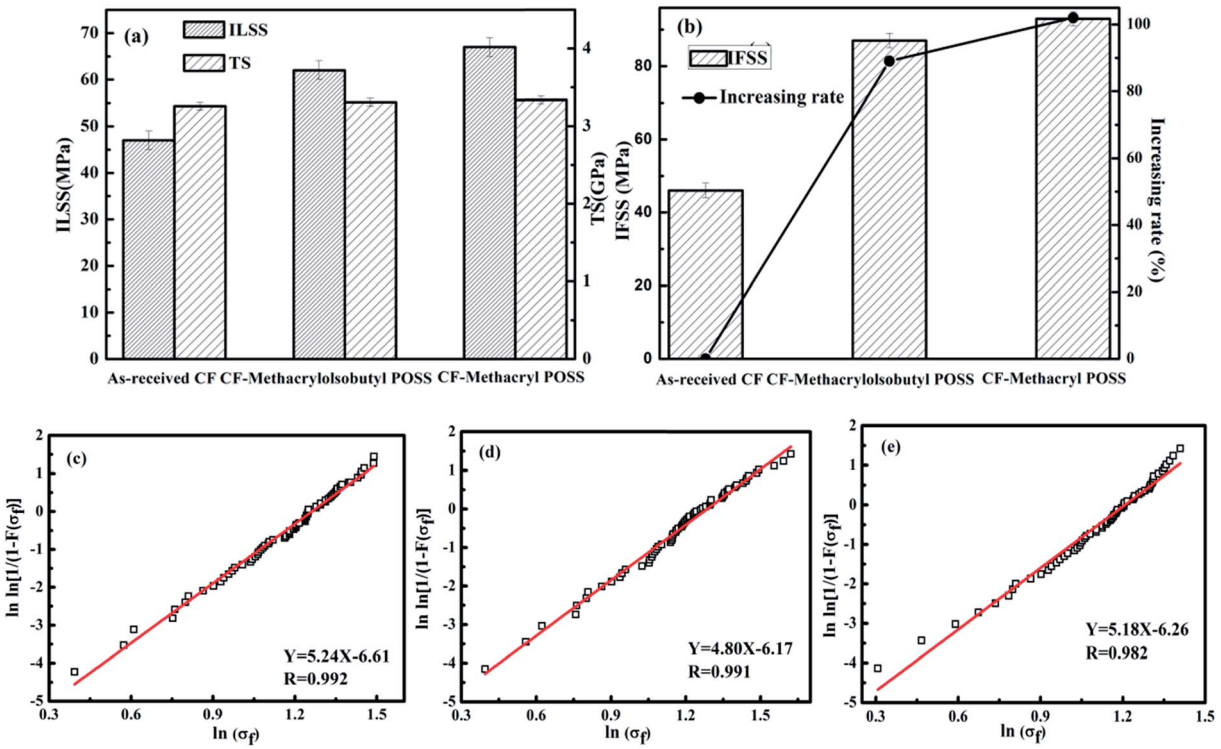

Fig. 7 (a) ILSS and TS, (b) IFSS and its increasing rate for composites reinforced with as-received, methacryl POSS grafted and methacrylolsobutyl grafted CFs, and the Weibull distribution plots of the (c) as-received single fibers, (d) methacrylolsobutyl POSS grafted single fibers, and (e) methacryl POSS grafted single fibers.

the UPR. As shown in Fig. 7(b), the IFSS of methacryl POSS grafted CFs is observed to have the highest value of 93 MPa, an increase of about 102.2% in comparison with the as-received CFs (46 MPa), and an increase by 6.2% compared with the methacrylolsobutyl POSS grafted CFs (87 MPa). The possible mechanisms of the improved IFSS might be related to the increased chemical bonding between nanofillers and the matrix.[47] In this work, the most important factor should be the chemical bonding in the interface region between CFs and UPR. Fig. S1† shows the illustration of a single fiber-micro-bond test. If debonding occurred at the interface of the methacryl POSS grafted CF reinforced UPR composites, the applied force would overcome both the fiber–resin adhesion strength and the chemical bonding in the interface region of CFs and UPR, Fig. S1† and Fig. 7(b), indicating a significantly improved interfacial interaction after CFs were grafted with methacryl POSS.

The influence of the grafted POSS on the tensile strength of the fibers was evaluated by single fiber tensile testing. The tensile strength of the as-received, methacryl and methacrylolsobutyl POSS grafted single carbon fiber follows the Weibull distribution plots, Fig. 7(c–e). The Weibull distribution, widely used in the failure behavior analysis, especially for brittle materials, is based on the series model of weakest link theorem. The basic equations (eqn (6–11)) for the model are shown as follows.[50]

$$F(\sigma_f) = 1 - \exp[-L(\sigma_f/\sigma_0)^{\beta}] \quad (6)$$

$F(\sigma_f)$ is the probability of failure, L is the reference length, β is the Weibull shape parameter for lifetime, σ_f is the tensile strength of a single fiber and σ_0 is the scale parameter. Both σ_0 and β are the material constants. All the parameters are determined based on the data obtained from the stress rupture testing.

$$P = 1 - F(\sigma_f) = \exp[-L(\sigma_f/\sigma_0)^{\beta}] \quad (7)$$

where P is the probability of survival. For the Weibull distribution, natural logarithm on both sides was used as in eqn (8).

$$\ln \ln[1/(1 - F(\sigma_f))] = \beta \ln \sigma_f + \ln L - \ln {\sigma_0}^{\beta} \quad (8)$$

where the $F(\sigma_f)$ is obtained by eqn (9).

$$F(\sigma_f) = x/(N + 1) \quad (9)$$

where N is the total fibers, and x is the fracture number of the fibers under the tensile stress. The tested strengths of the fibers are arranged sequentially in an ascending order as $\sigma_1 < \sigma_2 < \cdots \leq \sigma_i \leq \cdots \leq \sigma_x$, where σ_i is any of these tested strengths. When eqn (8) is rearranged as linear, $Y = [1/(1 - F(\sigma_f))]$, $B = \beta$, $X = \ln \sigma_f$, $A = \ln L - \ln {\sigma_0}^{\beta}$ is written. The linear equation $Y = A + BX$ can be obtained from curve fitting of $[1/(1 - F(\sigma_f))]$ and $\ln \sigma_f$. According to the B and A of the linear equation, σ_0 and $\beta = B$ are obtained.

$$\sigma_0 = \exp(\ln((\ln L - A)/\beta)) \quad (10)$$

The statistical average intensity $\bar{\alpha}_f$ can be obtained by eqn 11.

$$\bar{\alpha}_f = \sigma_0 L^{-1/\beta} \Gamma(1 + 1/\beta) \quad (11)$$

where $\Gamma()$ is the Gamma function.

The single fiber tensile strength test is usually performed to assess the influence of grafting modification on the tensile strength of the fibers. The Weibull distribution is a continuous probability distribution and an appropriate method to deal with the strength of many fibers. The strength of a single carbon fiber obeys the single Weibull distribution, *i.e.*, the lower the Weibull shape parameter is, the more defects the fibers have. Oxidation and grafting treatment will unavoidably introduce defects on the surface of fibers, which could decrease the fiber strength. However, compared with the strength of the as-received CFs (3.26 GPa), a comparable fiber tensile strength is observed for the CFs grafted with methacrylolsobutyl POSS (3.31 GPa) and for the CFs grafted with methacryl POSS (3.34 GPa), suggesting that the chemical grafting of POSS on the fibers has no significant effects on the fiber tensile strength. The results of single fiber tensile testing imply that the functionalization would not lead to any discernible decrease in the in-plane properties of the resulting composites.

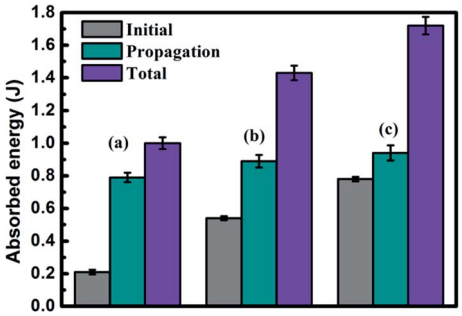

Fig. 8 Impact test of the composites reinforced with (a) as-received CFs, (b) methacrylolsobutyl POSS grafted CFs, and (c) methacryl POSS grafted CFs.

The impact toughness properties of the composites are largely affected by the interface region between CFs and the UPR matrix. But not all interfacial bonding can result in a satisfactory overall performance since the imperfect interface affects the mechanical properties of composites. Both weak and strong interfaces are not beneficial to the impact toughness of the composites, the detailed mechanism for the interface to affect the impact toughness was studied by Liu *et al.*[51] A moderate interface was revealed to improve the ILSS and impact properties at the same time. Fig. 8 shows the impact property testing results of the composites reinforced by the as-received CFs and POSS grafted CFs. The initial, propagative, and total absorbed energy of the as-received CF composites were 0.21, 0.79 and 1.00 J, respectively. After modification, the impact toughness was increased significantly for the composites containing methacrylolsobutyl POSS and methacryl POSS grafted CFs, respectively. The results indicate a higher impact strength than that without POSS grafted CFs. The initial, propagative, and total

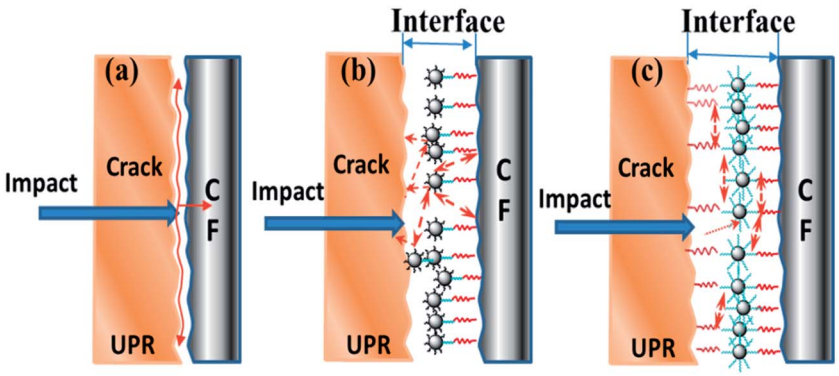

Fig. 9 Schematic of the impact test of the composites reinforced with (a) as-received CFs, (b) methacrylolsobutyl POSS grafted CFs, and (c) methacryl POSS grafted CFs.

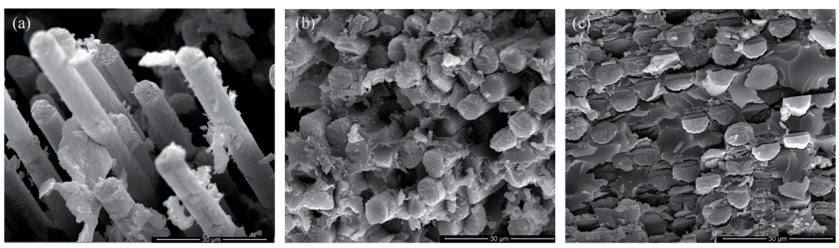

Fig. 10 Morphologies of the fractured surface of the UPR composites reinforced with (a) untreated CFs; (b) methacrylolsobutyl POSS grafted CFs, and (c) methacryl POSS grafted CFs.

absorbed energy were 0.94, 0.78 and 1.72 J for the composites with CFs grafted with methacryl POSS, respectively. The initial, propagative, and total absorbed energy was evidently improved compared with the composites with CFs grafted with methacrylolsobutyl POSS (0.54, 0.89 and 1.43 J), indicating that the presence of methacryl POSS has a better interface than the presence of methacrylolsobutyl POSS. The schematic illustration of the interphase of methacryl POSS and methacrylolsobutyl POSS grafted CFs/UPR composites is shown in Fig. 9. When an impact force is applied to the composites, the interface between CFs and UPR matrix serving as a shielding layer can induce more cracks to prevent the crack tips to directly touch the CF reinforcement that can efficiently absorb the fracture energy, resulting in an increased initial absorbed energy.

The impact fracture surface of the composites was investigated to better understand the interfacial bonding between CFs and the UPR matrix, Fig. 10(a–c). For the as-received CFs/UPR composites, Fig. 10(a), a large number of fibers were pulled out from the UPR matrix in a large area and the interface debonding between CFs and the UPR matrix was observed obviously, and big holes remained in the matrix, indicating a weak interfacial adhesion. This brittle fracture and lowest impact toughness have similar results to those of the glass fiber reinforced vinyl ester composites.[52] After grafting with methacrylolsobutyl POSS, a few fibers were pulled out and the pull-out length of the fibers was very short due to the increased roughness and wettability of the CFs, further confirming an improved interface between CFs and the UPR matrix, consistent with the FMAFM, IFSS and ILSS test.

Comparatively, the interface strength of the grafted methacryl POSS CF reinforced UPR composites was observed to be dramatically improved between CFs and the UPR matrix. No fiber pullout and fiber/matrix debonding were observed. The resin and fiber fragments were observed to be uniformly scattered on the fracture surface after being fractured by a powerful impulsion force. Nevertheless, the interface of the fiber and the matrix remains closely integrated together, indicating that there is a better interface in the grafted methacryl POSS CF reinforced UPR composites than that of the grafted methacrylolsobutyl POSS CF reinforced UPR composites. The further improved interfacial strength of the grafted methacryl POSS CF reinforced UPR composites is attributed to the chemical bonding at the interface of the composites, otherwise the fractured surface should be similar to that of the grafted methacrylolsobutyl POSS CF reinforced UPR composites with a comparable roughness and wettability. Therefore, the chemical bonding at the interface of the composites plays the most important role among the three factors that affect the interface of composites, *i.e.*, roughness, wettability and chemical bonding of the CF surface.

Conclusions

Through silanization with a coupling agent, both methacryl and methacrylolsobutyl POSS were uniformly grafted on the CF surface and effectively improved the interfacial adhesion between CFs and the UPR matrix. The wettability and roughness of the CFs grafted with both kinds of POSS were almost the same, while higher than that of the as-received CFs. For the UPR composites reinforced with methacryl POSS (multifunctional) grafted CFs, the ILSS, IFSS and the impact energy were dramatically increased compared with that of the UPR composites reinforced with methacrylolsobutyl POSS (monofunctional) grafted CFs. The ILSS, IFSS and impact energy of the UPR composites reinforced with methacryl POSS grafted CFs were 67, 93 MPa and 1.72 J, respectively, much higher than those of the UPR composites reinforced with methacrylolsobutyl POSS grafted CFs (62, 87 MPa and 1.43 J). Moreover, from the FMAFM and SEM observations of the impact fracture surfaces, the interfacial adhesion between the CFs grafted with methacryl POSS and the resin was also much better than that between the CFs grafted with methacrylolsobutyl POSS and the resin. The further improved interfacial strength for the methacryl POSS grafted CFs/UPR composites was attributed to two factors: (1) the enhanced mechanical interlocking and (2) the chemical bonding on the interface, and only mechanical locking existing on the interface of methacrylolsobutyl POSS grafted CFs/UPR composites. The chemical bonding at the interface of CFs/UPR composites was observed to play the most important role compared with other factors, *i.e.*, roughness and wettability, in enhancing the interface strength to improve the mechanical properties of the CFs/UPR composites.

Acknowledgements

The authors would like to thank the Chang Jiang Scholars Program and the National Natural Science Foundation of China (nos 51073047, 51173032 and 51303040) for financial support. Z. Guo acknowledges the National Science Foundation, (NSF, CMMI 10–30755 and 13–14486) USA.

References

1 L. Ci, J. Suhr, V. Pushparaj, X. Zhang and P. Ajayan, *Nano Lett.*, 2008, **8**, 2762–2766.
2 W.-H. Liao, H.-W. Tien, S.-T. Hsiao, S.-M. Li, Y.-S. Wang, Y.-L. Huang, S.-Y. Yang, C.-C. M. Ma and Y.-F. Wu, *ACS Appl. Mater. Interfaces*, 2013, **5**, 3975–3982.
3 T. Ogasawara, Y. Ishida and T. Kasai, *Compos. Sci. Technol.*, 2009, **69**, 2002–2007.
4 C. Jang, T. E. Lacy, S. R. Gwaltney, H. Toghiani and C. U. Pittman Jr, *Polymer*, 2013, **54**, 3282–3289.
5 K. Kepple, G. Sanborn, P. Lacasse, K. Gruenberg and W. Ready, *Carbon*, 2008, **46**, 2026–2033.
6 X. Shen, K. Li, H. Li, H. Du, W. Cao and F. Lan, *Carbon*, 2010, **48**, 344–351.
7 Y. Li, Q. Peng, X. He, P. Hu, C. Wang, Y. Shang, R. Wang, W. Jiao and H. Lv, *J. Mater. Chem.*, 2012, **22**, 18748–18752.
8 S. Chand, *J. Mater. Sci.*, 2000, **35**, 1303–1313.
9 M. Choi, B. Jeon and I. Chung, *Polymer*, 2000, **41**, 3243–3252.
10 M. Delamar, G. Desarmot, O. Fagebaume, R. Hitmi, J. Pinsonc and J.-M. Savéant, *Carbon*, 1997, **35**, 801–807.

11 G. J. Ehlert and H. A. Sodano, *ACS Appl. Mater. Interfaces*, 2009, **1**, 1827–1833.
12 Z. Xu, L. Chen, B. Zhou, Y. Li, B. Li, J. Niu, M. Shan, Q. Guo, Z. Wang and X. Qian, *RSC Adv.*, 2013, **3**, 10579–10597.
13 X. Zhang, Y. Song and Y. Huang, *Compos. Sci. Technol.*, 2007, **67**, 3014–3022.
14 H. Guo, Y. Huang, L. Liu and X. Shi, *Mater. Des.*, 2010, **31**, 1186–1190.
15 G. J. Ehlert, U. Galan and H. A. Sodano, *ACS Appl. Mater. Interfaces*, 2013, **5**, 635–645.
16 F. Zhao, Y. Huang, L. Liu, Y. Bai and L. Xu, *Carbon*, 2011, **49**, 2624–2632.
17 J. Zhu, S. Wei, J. Ryu, M. Budhathoki, G. Liang and Z. Guo, *J. Mater. Chem.*, 2010, **20**, 4937–4948.
18 V. Le Bonheur and S. I. Stupp, *Chem. Mater.*, 1993, **5**, 1287–1292.
19 A. Godara, L. Mezzo, F. Luizi, A. Warrier, S. V. Lomov, A. Van Vuure, L. Gorbatikh, P. Moldenaers and I. Verpoest, *Carbon*, 2009, **47**, 2914–2923.
20 F. Zhao and Y. Huang, *J. Mater. Chem.*, 2011, **21**, 2867–2870.
21 J. F. Timmerman, B. S. Hayes and J. C. Seferis, *Compos. Sci. Technol.*, 2002, **62**, 1249–1258.
22 A. B. Cherian, L. A. Varghese and E. T. Thachil, *Eur. Polym. J.*, 2007, **43**, 1460–1469.
23 X. Cao and L. J. Lee, *Polymer*, 2003, **44**, 1893–1902.
24 Z. Wu, L. Meng, L. Liu, Z. Jiang, L. Xing, D. Jiang and Y. Huang, *J. Adhes. Sci. Technol.*, 2014, **28**, 444–453.
25 H. W. Milliman, H. Ishida and D. A. Schiraldi, *Macromolecules*, 2012, **45**, 4650–4657.
26 C. Ramírez, M. Rico, A. Torres, L. Barral, J. López and B. Montero, *Eur. Polym. J.*, 2008, **44**, 3035–3045.
27 N. C. Escudé and E. Y.-X. Chen, *Chem. Mater.*, 2009, **21**, 5743–5753.
28 A. Fina, D. Tabuani, F. Carniato, A. Frache, E. Boccaleri and G. Camino, *Thermochim. Acta*, 2006, **440**, 36–42.
29 H.-U. Kim, Y. H. Bang, S. M. Choi and K. H. Yoon, *Compos. Sci. Technol.*, 2008, **68**, 2739–2747.
30 D. Jiang, L. Liu, J. Long, Y. Huang, Z. Wu, X. Yan and Z. Guo, *Compos. Sci. Technol.*, 2014, **100**, 158–165.
31 M. Seino, W. Wang, J. E. Lofgreen, D. P. Puzzo, T. Manabe and G. A. Ozin, *J. Am. Chem. Soc.*, 2011, **133**, 18082–18085.
32 Q. Wu, M. Bhattacharya and S. E. Morgan, *ACS Appl. Mater. Interfaces*, 2013, **5**, 6136–6146.
33 G. Z. Li, L. Wang, H. Toghiani, T. L. Daulton, K. Koyama and C. U. Pittman, *Macromolecules*, 2001, **34**, 8686–8693.
34 S.-W. Kuo and F.-C. Chang, *Prog. Polym. Sci.*, 2011, **36**, 1649–1696.
35 R. C. Bansal and M. Goyal, *Activated carbon adsorption*, CRC press, 2010.
36 G. Zhang, S. Sun, D. Yang, J.-P. Dodelet and E. Sacher, *Carbon*, 2008, **46**, 196–205.
37 X. Zhang, O. Alloul, Q. He, J. Zhu, M. J. Verde, Y. Li, S. Wei and Z. Guo, *Polymer*, 2013, **54**, 3594–3604.
38 Q. Peng, Y. Li, X. He, H. Lv, P. Hu, Y. Shang, C. Wang, R. Wang, T. Sritharan and S. Du, *Compos. Sci. Technol.*, 2013, **74**, 37–42.
39 Y. Luo, Y. Zhao, Y. Duan and S. Du, *Mater. Des.*, 2011, **32**, 941–946.
40 H. Qian, A. Bismarck, E. S. Greenhalgh, G. Kalinka and M. S. Shaffer, *Chem. Mater.*, 2008, **20**, 1862–1869.
41 T. Fukuma, M. J. Higgins and S. P. Jarvis, *Phys. Rev. Lett.*, 2007, **98**, 106101.
42 S.-i. Yamamoto and H. Yamada, *Langmuir*, 1997, **13**, 4861–4864.
43 F.-B. Li, G. Thompson and R. Newman, *Appl. Surf. Sci.*, 1998, **126**, 21–33.
44 D. Jiang, L. Liu, F. Zhao, Q. Zhang, S. Sun, J. He, B. Jiang and Y. Huang, *Fibers Polym.*, 2014, **15**, 566–573.
45 R. B. Pipes and N. Pagano, *J. Compos. Mater.*, 1970, **4**, 538–548.
46 E. Bekyarova, E. Thostenson, A. Yu, H. Kim, J. Gao, J. Tang, H. Hahn, T.-W. Chou, M. Itkis and R. Haddon, *Langmuir*, 2007, **23**, 3970–3974.
47 X. Zhang, X. Fan, C. Yan, H. Li, Y. Zhu, X. Li and L. Yu, *ACS Appl. Mater. Interfaces*, 2012, **4**, 1543–1552.
48 M. Li, R. Matsuyama and M. Sakai, *Carbon*, 1999, **37**, 1749–1757.
49 E. Bekyarova, E. T. Thostenson, A. Yu, M. E. Itkis, D. Fakhrutdinov, T.-W. Chou and R. C. Haddon, *J. Phys. Chem. C*, 2007, **111**, 17865–17871.
50 R. Sakin and I. Ay, *Mater. Des.*, 2008, **29**, 1170–1181.
51 P. Liu and Y. Yang, *Appl. Compos. Mater.*, 2014, 1–13.
52 L. Liao, X. Wang, P. Fang, K. M. Liew and C. Pan, *ACS Appl. Mater. Interfaces*, 2011, **3**, 534–538.